

This is an Open Access document downloaded from ORCA, Cardiff University's institutional repository: <https://orca.cardiff.ac.uk/id/eprint/116191/>

This is the author's version of a work that was submitted to / accepted for publication.

Citation for final published version:

Metters, Owen J., Forrest, Sebastian J. K., Sparkes, Hazel A., Manners, Ian and Wass, Duncan F. 2016. Small molecule activation by intermolecular Zr(IV)-phosphine frustrated Lewis pairs. *Journal of the American Chemical Society* 138 (6) , pp. 1994-2003. 10.1021/jacs.5b12536

Publishers page: <http://dx.doi.org/10.1021/jacs.5b12536>

Please note:

Changes made as a result of publishing processes such as copy-editing, formatting and page numbers may not be reflected in this version. For the definitive version of this publication, please refer to the published source. You are advised to consult the publisher's version if you wish to cite this paper.

This version is being made available in accordance with publisher policies. See <http://orca.cf.ac.uk/policies.html> for usage policies. Copyright and moral rights for publications made available in ORCA are retained by the copyright holders.

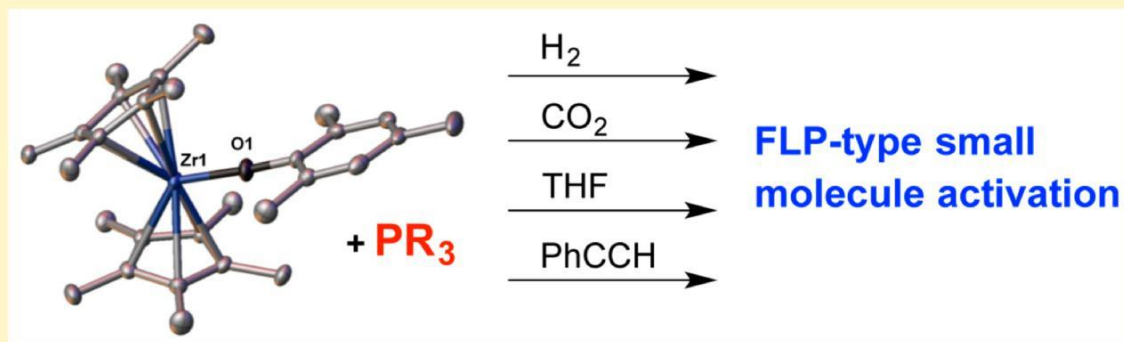


Small Molecule Activation by Intermolecular Zr(IV)-Phosphine Frustrated Lewis Pairs

Owen J. Metters, Sebastian J. K. Forrest, Hazel A. Sparkes, Ian Manners, and Duncan F. Wass*

School of Chemistry, University of Bristol, Cantock's Close, Bristol BS8 1TS, United Kingdom

* Supporting Information



ABSTRACT: We report intermolecular transition metal frustrated Lewis pairs (FLPs) based on zirconocene aryloxide and phosphine moieties that exhibit a broad range of small molecule activation chemistry that has previously been the preserve of only intramolecular pairs. Reactions with D₂, CO₂, THF, and PhCCH are reported. By contrast with previous intramolecular examples, these systems allow facile access to a variety of steric and electronic characteristics at the Lewis acidic and Lewis basic components, with the three-step syntheses of 10 new intermolecular transition metal FLPs being reported. Systematic variation to the phosphine Lewis base is used to unravel steric considerations, with the surprising conclusion that phosphines with relatively small Tolman steric parameters not only give highly reactive FLPs but are often seen to have the highest selectivity for the desired product. DOSY NMR spectroscopic studies on these systems reveal for the first time the nature of the Lewis acid/ Lewis base interactions in transition metal FLPs of this type.

1. INTRODUCTION

Frustrated Lewis pairs (FLPs) have proved to be a powerful new concept in small molecule activation and catalysis. By controlling the steric and electronic architecture of certain combinations of Lewis acids and bases to preclude the formation of a classical Lewis adduct, a high latent reactivity is imparted on the system.¹ This donor-acceptor ability is reminiscent of transition metal chemistry, and the ability of main group FLP systems to mimic reactivity normally associated with transition metals has been one of the remarkable features of this area. Initial investigations focused on the use of phosphine-borane FLPs and their ability to heterolytically cleave dihydrogen and facilitate hydrogenation reactions,² in addition to the binding and activation of carbon dioxide (CO₂).³ Subsequently, it was shown that main group FLPs are also able to mediate a wider range of transformations, such as 1,2-addition to alkynes⁴ and the ring opening of cyclic ethers.⁵

A wide selection of inter- and intramolecular main group FLPs based on diverse Lewis acid and base groups has now been reported.⁶⁻⁸ These pairs are able to mediate the heterolytic cleavage of H₂, CO₂ and isocyanate sequestration and deprotonation or 1,2 addition to terminal alkynes. Recent reports have also shown the utility of main group FLPs in

catalytic hydrogenation reactions. Intermolecular main group FLP systems are ubiquitous despite the obvious entropic disadvantages of this approach.

We, and others, have extended FLP chemistry to transition metals in the hope that combining the powerful small molecule activation chemistry of FLPs with the well-known suite of catalytically relevant reactions of transition metals could lead to yet more new chemistry.⁹ Much of our initial focus has been on intramolecular systems in which the fluorinated borane fragment is replaced by an electrophilic group 4 metallocene (Figure 1, A-C). The chemistry of these cationic zirconocene-phosphinoaryloxide complexes in general mirrors main group systems (activation of H₂, CO₂, THF), but also demonstrates reactivity that is either unique or rarely observed in main group systems, such as C-Cl and C-F bond cleavage, and catalytic dehydrocoupling of amine-boranes.¹⁰ Other related intramolecular zirconocene-phosphine systems have also been reported by Erker et al. (Figure 1, D and E). These compounds are accessed through 1,1- or 1,2-carbozirconation reactions of alkynes to the zirconium(IV) cation [Cp*₂ZrCH₃][B(C₆F₅)₄]. As with our intramolecular systems, these Zr/P pairs react with

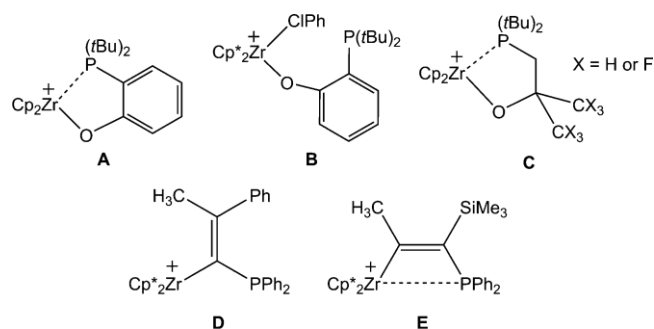
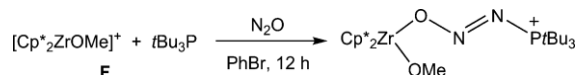


Figure 1. Intramolecular Zr/P FLPs developed by our group (A–C) and Erker et al. (D, E). In all cases, the $[\text{B}(\text{C}_6\text{F}_5)_4]^-$ counterion is omitted for clarity.

a multitude of small molecules (CO , CO_2 , H_2 , N_2 , O , $\text{PhC}(\text{H})\text{O}$, PhN , S , O),¹²

In stark contrast to the wide, varied and selective reactivity of these intramolecular FLPs, transformations mediated by intermolecular Zr/P FLPs are extremely limited. There are only two examples reported to date with the substrates employed limited to relatively reactive molecules containing highly polarized C–O or N–O bonds (example in Scheme 1).¹³ This very narrow reactivity is doubly disappointing in that

Scheme 1. Reactivity of an Intermolecular Zr/P FLP with N_2O



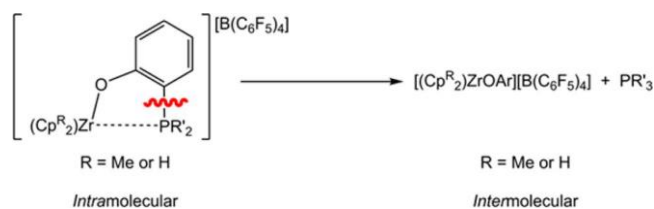
intermolecular systems offer the potential for more facile fine-tuning of electronic and steric parameters, for example, by using the wide range of commercially available phosphines, compared to the synthetically more challenging intramolecular analogues.

Certainly, an intermolecular system faces a more severe entropic challenge compared to its intramolecular analogue in bringing together three molecules. But the literature concerning main group FLPs is dominated by intermolecular systems, suggesting this should not be a fundamental impasse. Removal of the 1,2-aryl tether in our existing complexes (A–C) is an obvious way to design an intermolecular zirconocene aryloxide–phosphine FLP which could unlock this greater freedom in terms of tuning the steric and electronic properties of both the Lewis acidic electrophilic transition metal center and Lewis base (Scheme 2).

2. RESULTS AND DISCUSSION

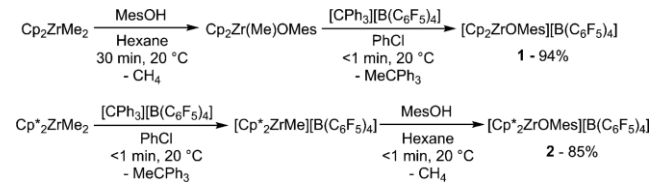
2.1. Synthesis of Cationic Zirconocene Aryloxide Lewis Acids. The required cationic Zr(IV) fragments shown in Scheme 2 were synthesized via two routes. The complex

Scheme 2. Removal of the Aryl Tether to Give an Intermolecular FLP



bearing Cp ligands was accessed through preparation of $[\text{Cp}_2\text{Zr}(\text{Me})\text{OMes}]$ ($-\text{OMes} = 2,4,6$ -trimethylphenoxide) by a modified literature procedure.¹⁴ Subsequent methyl abstraction using $[\text{CPh}_3][\text{B}(\text{C}_6\text{F}_5)_4]$ in a noncoordinating (PhCl) solvent gave $[\text{Cp}_2\text{ZrOMes}][\text{B}(\text{C}_6\text{F}_5)_4]$ (**1**) in 94% yield. The Cp^* analogue was synthesized by an alternative route, as protonolysis of a methyl group from Cp^*ZrMe_2 by 2,4,6-trimethylphenol (MesOH) was found to be extremely sluggish (60% yield after >10 days, 20 °C, hexane). $[\text{Cp}^*\text{ZrOMes}][\text{B}(\text{C}_6\text{F}_5)_4]$ (**2**) was therefore accessed by initial methyl abstraction from Cp^*ZrMe_2 using $[\text{CPh}_3][\text{B}(\text{C}_6\text{F}_5)_4]$ prior to protonolysis of the remaining methyl group using MesOH (Scheme 3). This modification afforded the desired complex in 85% yield over two steps in minutes.

Scheme 3. Synthesis of Zr(IV) Cations **1** and **2**^a



^aIsolated yields are shown where applicable.

The molecular structure of Zr(IV) cations **1** and **2** are shown in Figure 2. Complex **1** is stabilized by solvent coordination (chlorobenzene) in the solid state causing a slight bending of the Zr–O1–Mes bond angle (153.2(2)°). This is contrary to species **2**, which exhibits an essentially linear Zr1–O1–Mes angle (176.7(2)°) indicative of multiple Zr–O bonding. Solvent coordination in **2** is presumably precluded by the additional steric bulk afforded by the Cp^* ligand. In **2**, unlike in previously structurally characterized examples of cationic Zr–aryloxide complexes, there is no evidence of an agostic interaction between the *ortho*-alkyl group and the electron deficient zirconium.¹⁵

2.2. Reaction with Phosphines: Generation of Frustrated Lewis Pairs (FLPs). Taking our inspiration from main group systems and our previous intramolecular examples, initial attempts to generate an FLP system from **1** and **2** were made by addition of the bulky phosphine P^tBu_3 . However, this always

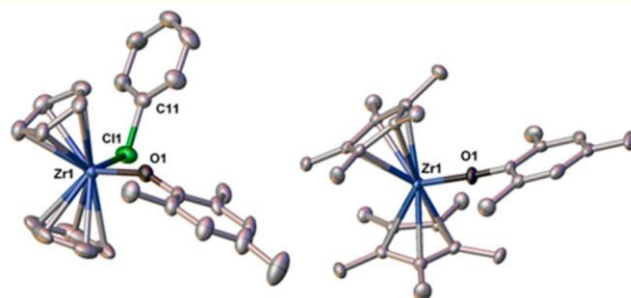


Figure 2. Molecular structure of **1** and **2** as determined by single crystal X-ray diffraction. Thermal ellipsoids are drawn at the 50% probability level. Hydrogens, $[\text{B}(\text{C}_6\text{F}_5)_4]^-$ counterion, and PhCl solvent of crystallization are omitted for clarity. Selected bond lengths (Å) and angles (deg): **1**: Zr1–O1 1.935(2), Zr1–C11 2.6630(8), Zr1–C11–C11 120.7(1), Zr1–O1–Mes 153.2(2), Cp–Zr–Cp 130.2(6). **2**: Zr1–O1 1.937(2), O1–Mes 1.368(4), Zr1–O1–Mes 176.7(2), $\text{Cp}^*\text{–Zr–Cp}^*$ 138.7(6).

resulted in an uncharacterizable mixture of products including appreciable amounts of $[\text{HP}^t\text{Bu}_3][\text{B}(\text{C}_6\text{F}_5)_4]$ (^{31}P NMR $\delta = 59.1$ ppm) which precluded further clean reactivity. By contrast, addition of an equimolar amount of a less basic and less sterically hindered phosphine (PCy_3 (a), PEt_3 (b), PPh_3 (c), PMes_3 (d), and $\text{P}(\text{C}_6\text{F}_5)_3$ (e)) to 1 and 2 in chlorobenzene solution resulted in clean conversion to new species.

In this case ^{31}P NMR spectroscopy is a useful probe for the nature of the Zr–P interaction, formation a Zr–P bond resulting in a large downfield shift (Table 1). In the case of 1, it

Table 1. ^{31}P NMR Chemical Shifts of Phosphines a–e and Lewis Pair Species 1a–e Correlated with the Relevant Tolman Steric Parameters (θ)

PR ₃	^{31}P NMR, δ/ppm	Zr/P	^{31}P NMR, δ/ppm	$\theta/^\circ$
PCy_3 (a)	8.8	1a	23.8	170
PEt_3 (b)	-19.2	1b	8.1	132
PPh_3 (c)	-5.0	1c	21.2	145
PMes_3 (d)	-36.5	1d	-36.5	212
$\text{P}(\text{C}_6\text{F}_5)_3$ (e)	-75.5	1e	-75.5	184

was found that upon addition of PCy_3 , PEt_3 , and PPh_3 , a Zr–P interaction was formed with 1a, 1b, and 1c all exhibiting large downfield shifts in their ^{31}P NMR resonances, when compared to the free phosphine. The systems containing the more bulky PMes_3 and $\text{P}(\text{C}_6\text{F}_5)_3$, 1d and 1e, show no change in their ^{31}P NMR chemical shift, suggestive of the absence of a Zr–P interaction. In contrast, none of the systems with the bulkier Cp^* complex 2 (2a–e) show evidence of a Zr–P interaction in solution. This pattern is in good agreement with the Tolman steric parameters of the phosphines as shown in Table 1,¹⁶ only the less bulky phosphines (with the less bulky zirconocene 1) possess a Zr–P interaction. The less basic nature of the fluoroaryl substituted phosphine is also likely to be an important electronic consideration.

A DOSY (Diffusion-Ordered Spectroscopy) NMR study was undertaken to detect potential secondary interactions present between the Lewis acid and Lewis base, but also to further explore the nature of the interaction present in 1a–c. A similar study has been carried out on main group $\text{PR}_3/\text{B}(\text{C}_6\text{F}_5)_3$ ($\text{R} = {}^t\text{Bu}$ and Mes) FLPs confirming secondary interactions are present between the fluorines on the $\text{B}(\text{C}_6\text{F}_5)_3$ and the protons on PR_3 .¹⁷ Our study shows that in 1a–c the interaction observed by ^{31}P NMR spectroscopy is in fact dynamic and not a persistent Zr–P bond. For example, under our conditions (0.06 mol dm^{-3} , $d_5\text{-PhBr}$),¹⁸ 1 was found to possess a diffusion coefficient (D) of $6.0 \times 10^{-10} \text{ m}^2 \text{ s}^{-1}$ and for PEt_3 (b) a value of $D = 19.5 \times 10^{-10} \text{ m}^2 \text{ s}^{-1}$. Upon combination of 1 with 1 equiv of PEt_3 to form 1b, the values of D obtained for the two components were found to be $5.5 \times 10^{-10} \text{ m}^2 \text{ s}^{-1}$ (1) and $7.3 \times 10^{-10} \text{ m}^2 \text{ s}^{-1}$ (PEt_3). The smaller diffusion coefficients in both cases indicate an interaction in solution consistent with the ^{31}P NMR spectrum, however if the interaction was a persistent Zr–P bond the values of D for the two components should be equal. The nature of the interaction is therefore dynamic, with the equilibrium positioned toward the “bound” pair. Similar observations were made in the case of 1a and 1c (data in the Supporting Information).

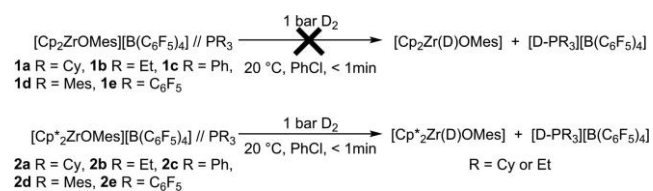
For FLP systems 1d–e and 2a–e, data obtained from DOSY experiments again shows the two components possessing smaller diffusion coefficients when in combination than when measured separately (Figures S15–S31). Taking 2b as an

example, the values of D for the separate components are $8.6 \times 10^{-10} \text{ m}^2 \text{ s}^{-1}$ (2) and $19.5 \times 10^{-10} \text{ m}^2 \text{ s}^{-1}$ (PEt_3), but upon combination these shift to $8.0 \times 10^{-10} \text{ m}^2 \text{ s}^{-1}$ (2) and $16.5 \times 10^{-10} \text{ m}^2 \text{ s}^{-1}$ (PEt_3 , (b)). This suggests again that a dynamic equilibrium may be present with encounter complexes forming and separating in solution. In this case, however, the increased steric bulk of the Cp^* ligands means that a classical metal–phosphine bond cannot form; therefore, the dynamic equilibrium must arise from other weaker secondary interactions perhaps between the ancillary ligands. In conclusion, the DOSY study does indicate some degree of preorganization of the FLP prior to further reactions.

2.3. Reactivity of Pairs with Dihydrogen (D_2). The heterolytic cleavage of H_2 is perhaps the most typical example of small molecule activation mediated by FLPs and was a logical starting point here. For experimental expedience, D_2 was used in place of H_2 to allow more precise monitoring by ^2H NMR spectroscopy.

When PhCl solutions of 1a–e were pressurized with 1 bar D_2 no reaction was observed (Scheme 4). This is consistent with

Scheme 4. Reactivity of FLP Systems 1a–e and 2a–e with 1 bar D_2



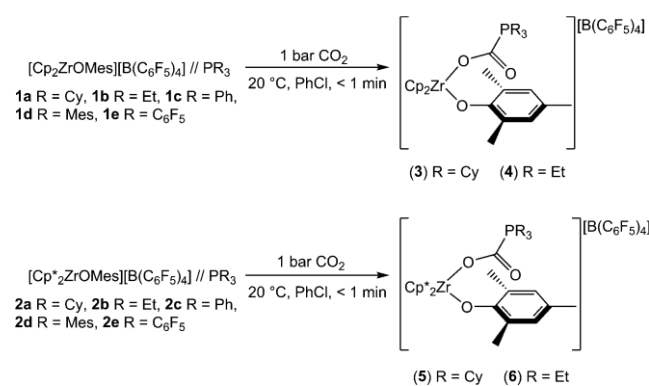
previous work where intramolecular Zr–P FLP systems bearing the Cp ligand set showed no reaction with H_2 under similar conditions. Previous work has indicated the necessity for at least one Cp^* ligand to achieve heterolytic hydrogen cleavage, attributed to the more electron rich ligand facilitating transient binding of H_2 to the Zr metal center and allowing deprotonation of this now more acidic species by the internal phosphine base. Consistent with this previous observation, 2a and 2b both showed an instantaneous reactions with 1 bar D_2 . In the case of 2a, a new species is observed by ^{31}P NMR spectroscopy ($\delta = 33.7$ ppm, $^1\text{J}_{\text{PD}} = 67$ Hz) displaying a characteristic 1:1:1 splitting pattern indicative of the formation of a P–D bond. The ^2H NMR spectrum confirms this assignment, with a doublet ($\delta = 4.25$ ppm, $^1\text{J}_{\text{PD}} = 67$ Hz) corresponding to the phosphonium deuteron and a sharp singlet ($\delta = 5.96$ ppm) assigned as the Zr–deuteride. Treatment of 2b with 1 bar D_2 results in a similar downfield shift in the ^{31}P NMR spectrum to give a 1:1:1 triplet again symptomatic of a P–D bond ($\delta = 21.1$ ppm, $^1\text{J}_{\text{PD}} = 67$ Hz). Species 2c–e display no reactivity under the same conditions, with the lower basicity of these aryl-substituted phosphines being our working hypothesis for this observation.

In an attempt to probe the mechanism of the hydrogen cleavage reaction, a chlorobenzene solution of 2 was pressurized with D_2 and cooled to -35°C , at which point no evidence for a Zr– D_2 complex was evident. These findings suggest a mechanism akin to that proposed by computational studies carried out on main-group FLP systems, in particular $\text{P}^t\text{Bu}_3/\text{B}(\text{C}_6\text{F}_5)_3$. In this case, it is proposed that preorganization of the FLP occurs prior to activation of the H_2 . This is corroborated by our DOSY data discussed above which

indicates the presence of transient encounter complexes in solution.

2.4. Reactivity of Pairs with Carbon Dioxide (CO₂). A range of main group and transition metal-based FLPs have shown the ability to sequester CO₂.^{2,6-8} The pairs 1a-e and 2a-e were treated with CO₂ by pressurizing chlorobenzene solutions of the species with 1 bar CO₂. Upon pressurizing with CO₂, systems 1a and 1b showed quantitative conversion to new species assigned as the CO₂ activation product by ³¹P NMR spectroscopy (3 δ = 27.9 ppm, 4 δ = 28.0 ppm). Compound 1c was found to yield two new species upon treatment with 1 bar CO₂ with ³¹P NMR chemical shifts of 5.4 and 19.9 ppm, however the ¹³C NMR spectrum showed no evidence of the carbonyl carbon. 1d and 1e were found to be inactive in the activation of CO₂ (Scheme 5).

Scheme 5. Reactivity of FLP Systems 1a-e and 2a-e with 1 bar CO₂



2a and 2b also react rapidly and quantitatively with 1 bar CO₂ giving rise to new species observed in the ³¹P NMR spectrum at δ = 24.9 ppm (5) and δ = 24.1 ppm (6). As with 1c-e, 2c gives a mixture of products when treated with CO₂, with no carbonyl peak visible in the ¹³C NMR spectrum, and 2d and 2e display no reactivity (Scheme 5). It surprised us to some extent that the cleanest results were obtained with the relatively nonbulky alkyl phosphines a and b, even in the cases where a Zr-P interaction is observed (1a and 1b); this echoes more recent results with main group FLPs where a truly “frustrated” system has been shown to be unnecessary so long as the Lewis acid and base can act in a cooperative fashion under the reaction conditions. The moniker “Cooperative Lewis Pairs” would seem to be increasingly appropriate. This also corroborates the DOSY study on 1a and 1b, which found that the Zr-P interaction is dynamic and a small amount of unbound Zr and PR₃ are present in solution. It is thought to be these species that react to form the desired products.

Crystallization under 1 bar CO₂ allows isolation of X-ray quality crystals of 6 in low (<5%) isolated yield.¹⁹ The molecular structure of 6 is shown in Figure 3.

The solid state structure of 6 shows a slight lengthening of the Zr1-O2 bond length in comparison with 2 (1.962(2) Å vs 1.937(2) Å) indicative of a slight loss of the multiple bond character due to coordination of an additional ligand at the electron deficient Zr center. As expected, C30 appears to be tending toward sp² in character with values of 112.7(2)° and 117.8(2)° for the O3-C30-P1 and O2-C30-P1 angles, respectively, but a significantly larger angle (129.5(3)°) between O2-C30-O3 indicates that C30 retains some sp

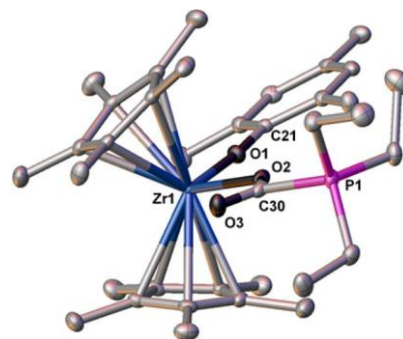
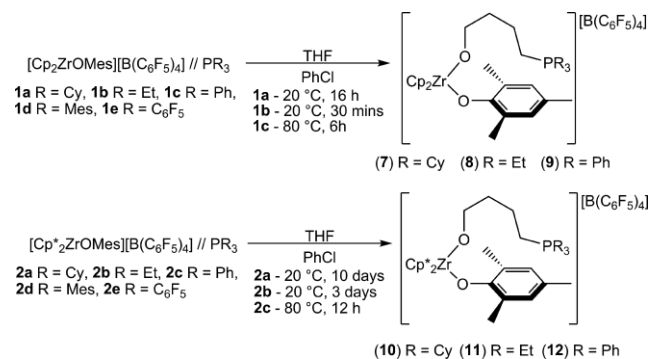


Figure 3. Molecular structure of 6 as determined by single crystal X-ray diffraction. Thermal ellipsoids are drawn at the 50% probability level. Hydrogens and the [B(C₆F₅)₄]⁻ counterion are omitted for clarity. Selected bond lengths (Å) and angles (deg): Zr1-O1 1.962(2), Zr1-O2 2.184(2), O2-C30 1.278(4), O3-C30 1.220(4), C30-P1 1.865(3), O2-C30-O3 129.5(3), O3-C30-P1 112.7(2), O2-C30-P1 117.8(2), Zr1-O1-C21 174.5(2), Zr1-O2-C30 129.1(2).

character. This is further reinforced by the only slightly longer C30-O2 bond length (1.278(4) Å) when compared to the C30-O3 double bond (1.220(4) Å).

2.5. Reactivity of Pairs with Tetrahydrofuran (THF). Treatment of chlorobenzene solutions of 1a-c with an excess of THF results in an immediate color change from orange to yellow and concomitant dissociation of the bound phosphine to yield what is proposed to be [Cp₂Zr(THF)OMes][B(C₆F₅)₄]. 1a reacts further to give quantitative conversion to 7 within 16h (³¹P NMR δ = 38.4 ppm), 1b undergoes a somewhat more rapid reaction to yield a species with a similar ³¹P NMR shift (³¹P NMR δ = 31.5 ppm) after 30 min assigned as 8. 1c shows no reaction at room temperature; however, upon heating to 80 °C for 6h full conversion to 9 is observed by ³¹P NMR spectroscopy (δ = 23.4 ppm). As with H₂ and CO₂, 1d and 1e show no further reaction with THF despite heating at 80 °C for 16 h (Scheme 6).

Scheme 6. Reactivity of FLP Systems 1a-e and 2a-e with THF



To further probe the mechanism of this reaction, postulated intermediate [Cp₂Zr(THF)OMes][B(C₆F₅)₄] (1-THF) has been synthesized and isolated by reaction of 1 with THF, the molecular structure of which is shown in Figure 4.

In comparison to 1, 1-THF shows a greater degree of bending of the Zr1-O1-Mes bond (139.8(8)° vs 153.2(2)°) in addition to a lengthening of the Zr1-O1 bond (1.972(1) Å vs 1.935(2) Å) due to the coordination of a more donating

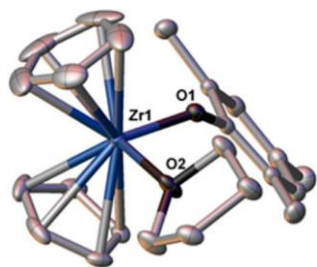


Figure 4. Molecular structures of 1-THF as determined by single crystal X-ray diffraction. Thermal ellipsoids are drawn at the 50% probability level. Disorder around the THF ligand, hydrogens, and the $[\text{B}(\text{C}_6\text{F}_5)_4]^-$ counterion are omitted for clarity. Selected bond lengths (Å) and angles (deg): Zr1–O1 1.972(1), Zr1–O2 2.206(1), Zr1–O1–Mes 139.8(8), O1–Zr1–O2 96.82(5).

ligand in the THF compared to chlorobenzene, thus further reducing the multiple bond character between the Zr and the aryloxy ligand.

Subsequent reaction of 1-THF with PR_3 (R = Cy, Et, Ph, Mes, C_6F_5) results in reactivity identical to that shown in Scheme 6. We can therefore propose that the reaction mechanism consists of an initial complexation of THF to the Lewis acidic zirconocene center, which activates the THF toward nucleophilic attack at the α -carbon by the phosphine. This mechanism fits well with the observed trend of the more nucleophilic phosphines giving more rapid reaction ($\text{PEt}_3 > \text{PCy}_3 > \text{PPh}_3 > \text{PMes}_3 > \text{P}(\text{C}_6\text{F}_5)_3$). Reaction of 1-THF with PEt_3 being significantly more rapid than with PCy_3 is thought to be a purely steric effect, with PEt_3 having a cone angle of 132° compared to 170° for PCy_3 . This mechanism is also consistent with works by Stephan et al. and Jordan et al., which describe the ring opening of Zr bound THF by phosphines and amines and independently conclude that the reaction proceeds by a Lewis acid activation of the C–O bond prior to nucleophilic attack at the α -carbon.²⁰

Similar, but overall less rapid reactivity is observed with 2a–e. Upon addition of excess THF to chlorobenzene solutions of 2a–e an immediate color change from red to yellow is observed indicating formation of a Zr–THF adduct as observed for 1a–e. 2-THF was isolated and characterized by the addition of THF to a chlorobenzene solution of 2, and the molecular structure is shown in Figure 5. An interesting structural feature of 2-THF is that, unlike its Cp analogue, the aryloxy ligand

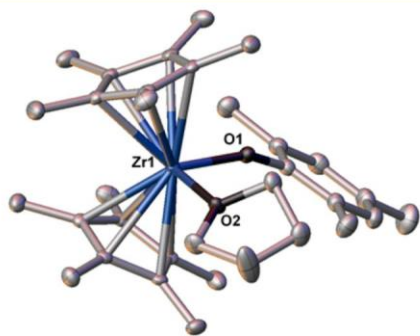


Figure 5. Molecular structure of 2-THF as determined by single crystal X-ray diffraction. Hydrogens, $[\text{B}(\text{C}_6\text{F}_5)_4]^-$ counterion, and solvent of crystallization are omitted for clarity. Selected bond lengths (Å) and angles (deg): Zr1–O1 1.984(1), Zr1–O2 2.282(1), O2–Zr1–O1 95.49(5), Zr1–O1–Mes 153.6(1).

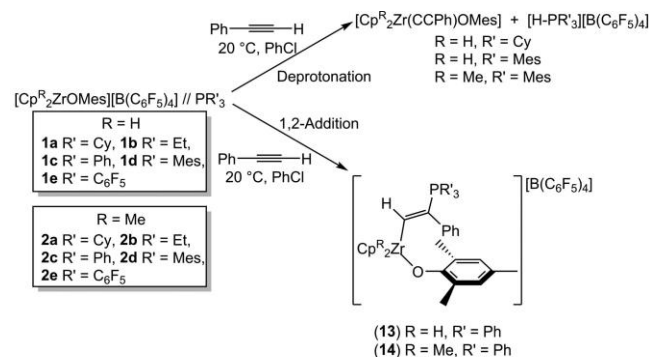
appears to be locked in conformation, with free rotation about the Zr1–O1–Mes axis precluded by the additional steric bulk. This is evidenced by the ^1H NMR spectra for the two species, wherein 1-THF is seen to possess two equivalent ortho- CH_3 groups ($\delta = 1.84$ ppm (broad)); however, in 2-THF, these become inequivalent ($\delta = 1.79$ and 1.88 ppm).

The solid-state structure of 2-THF also shows a significant bending of the Zr1–O1–Mes bond when compared to 2 (153.6(1) $^\circ$ vs 176.7(2) $^\circ$). This is accompanied by an extension of the Zr1–O1 bond upon binding of THF (1.937(2) to 1.984(1) Å) again indicating that binding of an additional donor ligand to the Zr center reduces the multiple bond character of the Zr1–O1 bond.

Analogous to compound 1a, species 2a reacts with an excess of THF at room temperature to yield 10 in 10 days (^{31}P NMR $\delta = 36.8$ ppm). Compound 2b again reacts significantly faster, proceeding to a >99% conversion to 11 in 3 days (^{31}P NMR $\delta = 30.2$ ppm). Compound 2c shows no reactivity with THF at room temperature, but upon heating to 80 $^\circ\text{C}$ complete conversion to 12 is observed within 12 h (^{31}P NMR $\delta = 21.9$ ppm). As with the system bearing the Cp ligand set, the analogous Cp* species 2d and 2e show no reaction with THF even at elevated temperature (80 $^\circ\text{C}$, 24h). This general trend of the ring opening of cyclic ethers proceeding less rapidly with 2a–e than 1a–e is proposed to be a steric effect with Cp* hindering the attack of the incoming phosphine nucleophile.

2.6. Reactivity of Pairs with Alkynes. The reaction of FLPs with terminal alkynes can proceed via one of two mechanisms, with the majority of main-group FLP systems going via a 1,2-addition reaction with the nature of the resulting isomer generally controlled by steric factors.⁴ However, in previous work with Zr/P FLPs, it has been shown that a deprotonation reaction may also take place yielding a zirconium acetylide and phosphonium species (Scheme 7).¹¹

Scheme 7. Reactivity of FLP Systems 1a–e and 2a–e with Phenylacetylene (PhCCH)



In the case of 1a, upon addition of phenylacetylene (PhCCH), clean deprotonation is observed to yield $[\text{HPCy}_3][\text{B}(\text{C}_6\text{F}_5)_4]$ (^{31}P NMR $\delta = 33.1$ ppm, $^1\text{J}_{\text{PH}} = 420$ Hz), and a zirconium acetylide complex. Surprisingly, compound 1b shows a change in selectivity, and when treated with PhCCH it undergoes a slow reaction (20 $^\circ\text{C}$, PhCl, 16 h) to yield a mixture of the two isomers of the 1,2-addition product (1:8). Separation of the isomers proved impossible due to their near identical solubility in a range of solvents. Reaction of 1c with PhCCH rapidly (20 $^\circ\text{C}$, PhCl, <1 min) yields the 1,2-addition product 13 ($^{31}\text{P}\{^1\text{H}\}$ NMR $\delta = 20.1$ ppm) with only the Zr/P trans isomer isolated. This was identified by comparison of the

^1H NMR spectra to the crystallographically characterized analogue 14 *vide infra*. In both cases, the alkenyl proton exhibits a $^3\text{J}_{\text{PH}}$ coupling of 45 Hz indicating an identical geometry around the double bond. A further change in selectivity is observed with 1d with the favored reaction pathway reverting back to deprotonation, such that upon treatment of 1d with PhCCH immediate formation of $[\text{H-PMes}_3][\text{B}(\text{C}_6\text{F}_5)_4]$ is detected by ^{31}P NMR spectroscopy (^{31}P NMR $\delta = -27.5$ ppm, $^1\text{J}_{\text{PH}} = 478$ Hz). Complex 1e exhibits no reaction with PhCCH. The pairs 2a–e exhibit a broadly similar trend in reactivity; however, both 2a and 2b yield a mixture of deprotonation and 1,2-addition products in ratios of 2:1 and 3:2, respectively. Again the system containing PPh₃, 2c, reacts cleanly and rapidly with PhCCH to generate only the 1,2-addition product 14 ($^{31}\text{P}\{^1\text{H}\}$ NMR $\delta = 17.4$ ppm), the molecular structure of which is shown in Figure 6. As is observed with 1d and 1e, 2d forms only the deprotonation product, $[\text{H-PMes}_3][\text{B}(\text{C}_6\text{F}_5)_4]$, and 2e does not react upon addition of PhCCH.

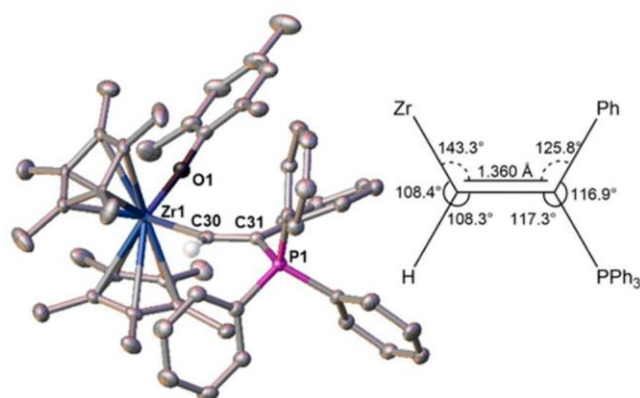


Figure 6. Molecular structure of 14 as determined by single crystal X-ray diffraction. Thermal ellipsoids are shown at the 50% probability level, and irrelevant hydrogens, $[\text{B}(\text{C}_6\text{F}_5)_4]^-$ counterion, and disorder around the Cp* rings are omitted for clarity. Inset is a representation of the C–C bond geometry. Selected bond lengths (Å) and angles (deg): Zr1–O1 1.971(2), Zr1–C30 2.327(3), C30–C31 1.360(3), P1–C31 1.815(3), O1–Zr1–C30 100.29(8), Zr1–O1–Mes 173.1(2), Zr1–C30–C31 143.3(2), C30–C31–Ph 125.8(2), Ph–C31–P1 116.9(2), P1–C31–C30 117.3(2).

The molecular structure of 14 (Figure 6) reveals the *trans*-Zr/P conformation with the Ph moiety of PhCCH geminal to PPh₃. This conformer is assumed to be preferred as it reduces steric clashes between the bulky Cp* ligands with the phenyl rings of both PPh₃ and PhCCH. C31 appears to possess a greater degree of sp^2 character when compared to C30 as evidenced by the large Zr1–C30–C31 angle ($143.3(2)^\circ$), this could again be attributed to the steric strain enforced by the interaction between the Ph group and the bulk aryloxide ligand on Zr.

These two competing reaction pathways have previously been observed by Erker et al., the main group FLP system $\text{P}^t\text{Bu}_3/\text{B}(\text{C}_6\text{F}_5)_3$ reacting with a terminal alkyne to give the deprotonation product, whereas $\text{PAr}_3/\text{B}(\text{C}_6\text{F}_5)_3$ ($\text{PAr}_3 = \text{P}(\text{o-tolyl})_3$ or $\text{P}\{\text{Ph}_2[2,5\text{-bis}(\text{trifluoromethyl})\text{phenyl}]\}$) cleanly yields the 1,2-addition product.^{4b} This reactivity can generally be attributed to electronic factors with the more basic phosphines favoring deprotonation; however, there may also be a steric effect as $\text{P}(\text{o-tolyl})_3$ and PMes_3 are considered to be

electronically similar, but have significantly different steric parameters, with cone angles of 194° and 212° , respectively. This could be responsible for the switch in reactivity from 1,2-addition ($\text{P}(\text{o-tolyl})_3$, Erker et al.) to deprotonation (PMes_3 , *vide supra*).

3. CONCLUSION

We have synthesized a range of intermolecular zirconium/phosphine FLPs derived from zirconocene cations and tertiary phosphines of varying steric and electronic properties. A DOSY NMR spectroscopic study on these systems has shown the nature of the Lewis acid/Lewis base interactions present in all cases. These pairs show for the first time the ability of intermolecular FLPs containing a transition metal fragment as the Lewis acid to react in an analogous fashion to their intramolecular counterparts.²¹ These new systems are shown to mediate the activation of a range of small molecules (D_2 , CO_2 , THF, phenylacetylene) with the reactivity toward these substrates highly dependent on the steric and electronic nature of the phosphine employed, a factor which had remained previously unexplored with transition metal FLPs. It has been found that the phosphine must be of sufficient basicity to promote such reactions; in all cases, systems using the weakly basic $\text{P}(\text{C}_6\text{F}_5)_3$ (1e and 2e) show no reactivity toward the small molecules studied. Given sufficient Lewis basicity, high steric bulk in the phosphine used is surprisingly unimportant; indeed, the least bulky phosphine used here, PET_3 , gives the cleanest results. In addition, the base used has a dramatic effect on selectivity, as evidenced by the switch in reaction mode with phenylacetylene from 1,2-addition to deprotonation when the less bulky PPh₃ (1c and 2c) is replaced with the significantly more bulky PMes_3 (1d and 2d). These results show that the use of intramolecular systems is not a prerequisite for transition metal FLPs and open many other possibilities for the design of intermolecular transition metal frustrated or cooperative Lewis pairs.

4. EXPERIMENTAL SECTION

4.1. General Considerations. Unless otherwise stated, all manipulations were undertaken under an atmosphere of argon or nitrogen using standard glovebox (M-Braun $\text{O}_2 < 0.1$ ppm, $\text{H}_2\text{O} < 0.1$ ppm) and Schlenk line techniques and all glassware were oven and vacuum-dried prior to use. Cp_2ZrCl_2 , $\text{Cp}^*_2\text{ZrCl}_2\text{MeLi}$ (1.6 M in Et_2O), PCy_3 , PET_3 , PPh_3 , PMes_3 , and $\text{P}(\text{C}_6\text{F}_5)_3$ were purchased from Sigma-Aldrich and used as received. $[\text{CPh}_3][\text{B}(\text{C}_6\text{F}_5)_4]$ was purchased from Acros Organics and used as received. 2,4,6-Trimethylphenol (MesOH) was purchased from Sigma-Aldrich and dried prior to use by stirring a hexane solution over CaH_2 before removal of the solvent in vacuo and sublimation (25°C , 2×10^{-2} Torr). Phenylacetylene was purchased from Sigma-Aldrich and purified by distillation before use. Reagent gases (D_2 and CO_2) were dried prior to use by passing through a -78°C trap. Cp_2ZrMe_2 and $\text{Cp}^*_2\text{ZrMe}_2$ were synthesized according to literature protocols.²² Common laboratory solvents (Et_2O , DCM, hexane, THF) were purified using a Grubbs type purification system.²³ Nonstandard solvents (chlorobenzene, pentane) were purchased from Sigma-Aldrich and distilled from CaH_2 prior to use.

NMR spectra were recorded using JEOL ECP-300 (300 MHz), Varian-400 (400 MHz), and Varian NMR500 (500 MHz) spectrometers. Deuterated solvents were obtained from Sigma-Aldrich (d_6 -benzene, d_8 -THF, and d_2 -DCM) or Apollo Scientific (d_5 -PhBr) and distilled from CaH_2 prior to use. Spectra of air sensitive compounds were recorded using NMR tubes fitted with J. Young valves.

X-ray diffraction experiments were carried out at 100 K on a Bruker APEX II diffractometer using Mo K α radiation ($\lambda = 0.71073 \text{ \AA}$). For further details, see the [Supporting Information](#).

Mass spectrometry experiments were carried out by the University of Bristol Mass Spectrometry Service on a Bruker Daltonics micrO TOF II with a TOF analyzer. All samples were run in predried PhCl.

4.2. Synthesis of Zr Lewis acids. Cp₂Zr(Me)OMes. Cp₂Zr(Me)-OMes was prepared by a modified literature procedure.¹⁴ Cp₂ZrMe₂ (630 mg, 2.5 mmol) was dissolved in hexane (30 mL), and a solution of 2,4,6-trimethylphenol (323 mg, 2.5 mmol) in hexane (10 mL) was added dropwise. Effervescence was observed, and the resulting solution was stirred for 1 h. The solvent was removed in vacuo to yield a white solid. Recrystallization from hexanes at $-78 \text{ }^\circ\text{C}$ gave a white crystalline solid (725 mg, 78%).

¹H NMR (300 MHz, CD₂Cl₂) δ 0.31 (3H, s, CH₃), 2.01 (6H, s, ortho-CH₃), 2.19 (3H, s, para-CH₃), 6.09 (10H, s, Cp), 6.73 (2H, s, aryl-H).

[Cp₂ZrOMes][B(C₆F₅)₄] (1). In a glovebox, a chlorobenzene (1 mL) solution of [CPh₃][B(C₆F₅)₄] (198 mg, 0.2 mmol) was added dropwise to a stirred chlorobenzene (1 mL) solution of Cp₂Zr(Me)-OMes (80 mg, 0.2 mmol). The orange solution was allowed to stir for 5 min before isolating the product via precipitation into a large volume (25 mL) of rapidly stirred hexane. The resulting yellow powder was washed with pentane (3 \times 5 mL) and dried in vacuo (204 mg, 94%).

¹H NMR (300 MHz, C₆D₆) δ 1.74 (6H, s, ortho-CH₃), 2.19 (3H, s, para-CH₃), 5.49 (10H, s, Cp) 6.76 (2H, s, Ar-H). ¹³C NMR (125 MHz, C₆D₆) δ 17.1 (s, ortho-CH₃), 20.5 (s, para-CH₃), 117.5 (s, Cp), 128.77 (s, ortho-C), 130.0 (s, meta-C), 130.3 (s, para-C), 131.9 (s, ipso-C). ESI-MS (+ve detection) 355.0629 m/z [Cp₂ZrOMes]⁺. Elem. Anal. Calcd (%): C, 49.87; H, 2.04. Found (%): C, 49.67; H, 2.63.

[Cp*₂ZrOMes][B(C₆F₅)₄] (2). In a glovebox, a chlorobenzene (1 mL) solution of [CPh₃][B(C₆F₅)₄] (94 mg, 0.1 mmol) was added dropwise to a stirred chlorobenzene solution of Cp*₂ZrMe₂ to give an orange solution. Upon dropwise addition of a chlorobenzene solution of 2,4,6-trimethylphenol (14 mg, 0.1 mmol), effervescence was observed accompanied by a color change from orange to deep red. After the effervescence had ceased (5 min), the product was isolated via precipitation into a large volume (25 mL) of rapidly stirred hexane. The resulting dark red powder was washed with pentane (3 \times 5 mL) and dried in vacuo (100 mg, 85%). Crystals of 2 suitable for analysis by single crystal X-ray diffraction were obtained by layering a chlorobenzene solution with pentane (3 days).

¹H NMR (300 MHz, d₅-PhCl) δ 1.63 (30H, s, Cp*), 1.72 (6H, s, ortho-CH₃), 2.20 (3H, s, para-CH₃), 6.79 (2H, s, Ar-H). ¹³C NMR (125 MHz, d₅-PhCl) δ 13.9 (s, Cp*-CH₃), 21.0 (s, ortho-CH₃), 23.6 (s, para-CH₃), 132.9 (s, Ar-CH), 137.1 (s, ipso-C). Other aryl carbons were obscured by PhCl peaks. ESI-MS (+ve detection) 495.2204 m/z [Cp*₂ZrOMes]⁺. Elem. Anal. Calcd (%): C, 54.14; H, 3.51. Found (%): C, 54.47; H, 3.80.

4.3. Generation of FLPs. [Cp₂ZrOMes][B(C₆F₅)₄] // PR₃ (1a-e). In a glovebox, a chlorobenzene (0.5 mL) solution of 1 (30 mg, 0.029 mmol) was added to a chlorobenzene (0.5 mL) solution of PR₃ (R = Cy (8.1 mg, 0.029 mmol), Et (3.4 mg, 0.029 mmol), Ph (7.6 mg 0.029 mmol), Mes (11.3 mg, 0.029 mmol), C₆F₅ (15.4 mg, 0.029 mmol)). Upon addition, a color change (orange to yellow) was observed for R = Cy, Et, and Ph, indicative of the presence of a Zr-P interaction.

For reaction of the FLP with substrates, the product was not isolated, but instead used in situ.

R = Cy. ³¹P NMR (121 MHz, PhCl) δ 24.3 (s, Zr-PCy₃). NB: PCy₃ δ = 8.8.

R = Et. ³¹P NMR (121 MHz, PhCl) δ 8.1 (s, Zr-PEt₃). NB: PEt₃ δ = -19.2.

R = Ph. ³¹P NMR (121 MHz, PhCl) δ 21.2 (s, Zr-PPh₃). NB: PPh₃ δ = -5.0.

R = Mes. ³¹P NMR (121 MHz, PhCl) δ -36.5 (s, PMes₃). NB: -36.5.PMes₃ δ =

R = C₆F₅. ³¹P NMR (121 MHz, PhCl) δ -75.5 (s, P(C₆F₅)₃). NB: P(C₆F₅)₃ δ = -75.5.

[Cp*₂ZrOMes][B(C₆F₅)₄] // PR₃ (2a-e). In a glovebox, a chlorobenzene (0.5 mL) solution of 2 (30 mg, 0.025 mmol) was

added to a chlorobenzene (0.5 mL) solution of PR₃ (R = Cy (7.1 mg, 0.025 mmol), Et (3.0 mg, 0.025 mmol), Ph (6.7 mg 0.025 mmol), Mes (9.9 mg, 0.025 mmol), C₆F₅ (14.0 mg, 0.025 mmol)). Upon addition, no change in color of ³¹P NMR chemical shift was observed. For reaction of the FLP with substrates, the product was not isolated, but instead used in situ.

4.4. DOSY Study of 1a-e and 2a-e. Samples of 1a-e and 2a-e and separate control samples of 1, 2, and PR₃ (R = Cy, Et, Ph, Mes, C₆F₅) were made as detailed above, but dissolved in d₅-PhBr. In the case of 1, 2, PR₃ (R = Cy, Et, Ph, Mes), 1a-d, and 2a-d, ¹H DOSY NMR spectroscopy experiments were carried out using 15 increments and a diffusion delay of 100 ms. For 1e, 2e, and P(C₆F₅)₃, the analogous experiment was carried out using ¹⁹F DOSY NMR spectroscopy due to the lack of protons on the P(C₆F₅)₃. The results of the study can be found in [Figures S15-S31](#): All data was analyzed using DOSY-Toolbox.²⁴

4.5. Reaction of Pairs with D₂. Reactivity of [Cp₂ZrOMes][B(C₆F₅)₄]//PR₃ (1a-e). In a glovebox, 1 (30 mg, 0.028 mmol) and an equimolar amount of the corresponding phosphine (0.028 mmol, a = PCy₃ (8.1 mg), b = PEt₃ (3.4 mg), c = PPh₃ (7.6 mg), d = PMes₃ (11.3 mg), e = P(C₆F₅)₃ (15.4 mg)) were weighed out and dissolved in PhCl (0.7 mL) before transferring to an NMR tube fitted with a J. Young valve. Following removal from the glovebox, the sample was subjected to a freeze-pump-thaw degassing cycle prior to refilling with 1 bar D₂. In all cases, no change in the ³¹P NMR spectra was observed following addition of D₂.

Reactivity of [Cp*₂ZrOMes][B(C₆F₅)₄]//PR₃ (2a-e). In a glovebox, 2 (30 mg, 0.026 mmol) and an equimolar amount of the corresponding phosphine (0.026 mmol, a = PCy₃ (7.1 mg), b = PEt₃ (3.0 mg), c = PPh₃ (6.7 mg), d = PMes₃ (9.9 mg), e = P(C₆F₅)₃ (14.0 mg)) were weighed out and dissolved in PhCl (0.7 mL) before transferring to an NMR tube fitted with a J. Young valve. Following removal from the glovebox, the sample was subjected to a freeze-pump-thaw degassing cycle prior to refilling with 1 bar D₂. In the case of 2a and 2b, an instantaneous color change from red to pale yellow was observed. Collected spectral data is detailed below:

2a + D₂. ³¹P NMR (121 MHz, PhCl) δ 33.6 (1:1:1 triplet, ¹J_{PD} = 68 Hz, [DPCy₃]⁺). ²H NMR (46 MHz, PhCl) δ 4.22 (d, ¹J_{PD} = 68 Hz, [DPCy₃]⁺), 5.98 (s, Zr-D).

2b + D₂. ³¹P NMR (121 MHz, PhCl) δ 21.2 (1:1:1 triplet, ¹J_{PD} = 68 Hz, [DPEt₃]⁺). ²H NMR (46 MHz, PhCl) δ 4.40 (v. broad, [DPCy₃]⁺), 5.98 (s, Zr-D).

4.6. Reaction of Pairs with CO₂. Reactivity of [Cp₂ZrOMes][B(C₆F₅)₄]//PR₃ (1a-e). In a glovebox, 1 (30 mg, 0.028 mmol) and an equimolar amount of the corresponding phosphine (0.028 mmol, a = PCy₃ (8.1 mg), b = PEt₃ (3.4 mg), c = PPh₃ (7.6 mg), d = PMes₃ (11.3 mg), e = P(C₆F₅)₃ (15.4 mg)) were weighed out and dissolved in PhCl (0.7 mL) before transferring to an NMR tube fitted with a J. Young valve. Following removal from the glovebox, the sample was subjected to a freeze-pump-thaw degassing cycle prior to refilling with 1 bar CO₂ via a $-78 \text{ }^\circ\text{C}$ trap. In the cases of 1a, 1b, and 1c, an immediate lightening of the yellow color was observed. In all cases, isolation under 1 bar CO₂ was attempted, but was not possible. As such all spectral data was obtained in situ.

Compound 3. ¹H NMR (500 MHz, PhCl) δ 1.60–1.81 (30H, m, PCy₃), 1.99 (6H, s, ortho-CH₃), 2.20 (3H, s, para-CH₃), 6.13 (10H, s, Cp), 6.76 (2H, s, Ar-H). ¹³C NMR (125 MHz, PhCl) δ 17.7 (s, ortho-CH₃), 20.3 (s, para-CH₃), 25.2 (s, para-C (PCy₃)), 26.4 (d, ³J_{PC} = 12 Hz, meta-C (PCy₃)), 26.9 (d, ²J_{PC} = 4 Hz, meta-C (PCy₃)), 30.7 (d, ¹J_{PC} = 33 Hz, ipso-C (PCy₃)), 114.7 (s, Cp), 123.3 (s, para-C), 124.6 (s, ortho-C), 160.4 (s, ipso-C), 162.5 (d, ¹J_{PC} = 100 Hz, C(O) O). NB: meta-C peak obscured by PhCl. ³¹P NMR (121 MHz, PhCl) δ 27.9 (s).

Compound 4. ¹H NMR (500 MHz, PhCl) δ 0.97 (9H, t, CH₃ (PEt₃)), 1.78 (6H, m, CH₂ (PEt₃)), 1.93 (6H, s, ortho-CH₃), 2.21 (3H, s, para-CH₃), 6.09 (10H, s, Cp), 6.76 (2H, s, Ar-H). ¹³C NMR (125 MHz, PhCl) δ 5.3 (d, ²J_{PC} = 5 Hz), 11.4 (d, ¹J_{PC} = 42 Hz), 17.3 (s, ortho-CH), 20.3 (s, para-CH), 114.9 (s, Cp), 123.3 (s, para-C),

124.6 (s, ortho-C), 160.3 (s, ipso-C), 162.4 (d, J_{PC} = 112 Hz, C(O)

O). NB: meta-C peak obscured by PhCl. ³¹P NMR (121 MHz, PhCl) δ 27.6 (s).

Reactivity of [Cp*₂ZrOMes][B(C₆F₅)₄]/PR₃ (2a-e). In a glovebox, 2 (30 mg, 0.026 mmol) and an equimolar amount of the corresponding phosphine (0.026 mmol, a = PCy₃ (7.1 mg), b = PEt₃ (3.0 mg), c = PPh₃ (6.7 mg), d = PMes₃ (9.9 mg), e = P(C₆F₅)₃ (14 mg)) were weighed out and dissolved in PhCl (0.7 mL) before transferring to an NMR tube fitted with a J. Young valve. Following removal from the glovebox, the sample was subjected to a freeze-pump-thaw degassing cycle prior to refilling with 1 bar CO₂ via a -78 °C trap. In the cases of 2a, 2b, and 2c, an immediate color change from red to yellow was observed. In all cases, isolation under 1 bar CO₂ was attempted, but was only possible in the case of 6 and in <5% yield. As such all spectral data was obtained in situ.

Compound 5. ¹H NMR (500 MHz, PhCl) δ 1.02 (9H, m, CH₃ (PEt₃)), 1.69 (30H, s, Cp*), 1.87 (6H, m, CH₂ (PEt₃)), 1.94 (3H, s, ortho-CH₃), 2.00 (3H, s, ortho-CH₃), 2.19 (3H, s, para-CH₃), 6.67 (2H, s, Ar-H). ¹³C NMR (125 MHz, PhCl) δ 11.7 (s, Cp*), 18.7 and 19.8 (s, ortho-CH₃), 20.1 (s, para-CH₃), 25.1 (s, para-C (PCy₃)), 26.5 (d, ³J_{PC} = 12 Hz, meta-C (PCy₃)), 27.2 (d, ²J_{PC} = 4 Hz, ortho-C (PCy₃)), 32.0 (d, ¹J_{PC} = 30 Hz, ipso-C (PCy₃)), 122.6 (s, Cp*), 124.1 (s, para-C), 124.6 (s, ortho-C), 156.4 (s, ipso-C), 161.6 (d, ¹J_{PC} = 92

Hz, C(O) O). NB: meta-C peak obscured by PhCl. ³¹P NMR (121 MHz, PhCl): δ 22.5 (s).

Compound 6. ¹H NMR (500 MHz, PhCl) δ 1.02 (9H, m, CH₃ (PEt₃)), 1.69 (30H, s, Cp*), 1.87 (6H, m, CH₂ (PEt₃)), 1.94 (3H, s, ortho-CH₃), 2.00 (3H, s, ortho-CH₃), 2.19 (3H, s, para-CH₃), 6.67 (2H, s, Ar-H). ¹³C NMR (125 MHz, PhCl) δ 5.4 (d, ²J_{PC} = 5 Hz), 11.3 (s, Cp*), 11.8 (d, ¹J_{PC} = 42 Hz), 18.1 and 19.6 (s, ortho-CH₃), 20.2 (s, para-CH), 122.4 (s, Cp*), 123.9 (s, para-C), 124.6 (s, ortho-

C), 156.2 (s, ipso-C), 161.6 (d, ¹J_{PC} = 108 Hz, C(O) O). NB: meta-C peak obscured by PhCl. ³¹P NMR (121 MHz, PhCl): δ 27.9 (s). 4.7.

Reaction of Pairs with THF. Reactivity of [Cp₂ZrOMes][B(C₆F₅)₄]/PR₃ (1a-e). In a glovebox, 1 (30 mg, 0.028 mmol) and an equimolar amount of the corresponding phosphine (0.019 mg, a = PCy₃ (8.1 mg), b = PEt₃ (3.4 mg), c = PPh₃ (7.6 mg), d = PMes₃ (11.3 mg), e = P(C₆F₅)₃ (15.4 mg)) were weighed out and dissolved in PhCl (0.7 mL) before transferring to an NMR tube fitted with a J. Young valve. The resulting solution was treated with five drops of THF, and a slight lightening of the yellow color observed. The ³¹P NMR spectrum of the solution indicated full conversion to free phosphine in all cases caused by its displacement by the THF moiety. When the reaction was deemed complete by ³¹P NMR spectroscopy, the product was isolated by precipitation into rapidly stirred hexane, washed with pentane (3 × 5 mL), and dried in vacuo.

Compound 7. Yield = 24 mg (60%). ¹H NMR (500 MHz, d₈-THF) δ 1.80–2.04 (34H, m, PCy₃, β-CH₂ and γ-CH₂), 2.10 (6H, s, ortho-CH₃), 2.21 (3H, s, para-CH₃), 2.28 (2H, m, δ-CH₂), 4.12 (2H, t, ³J_{HH} = 6 Hz, α-CH₂), 6.23 (10H, s, Cp), 6.69 (2H, s, Ar-H). ¹³C NMR (125 MHz, d₈-THF) δ 16.3 (d, ¹J_{PC} = 43 Hz, δ-CH₂), 18.2 (s, ortho-CH₃), 20.7 (d, ²J_{PC} = 5 Hz, γ-CH₂), 20.8 (s, para-CH₃), 23.3 (s, para-C (PCy₃)), 27.5 (d, ³J_{PC} = 12 Hz, meta-C (PCy₃)), 27.8 (d, ²J_{PC} = 4 Hz, ortho-C (PCy₃)), 30.8 (d, ¹J_{PC} = 42 Hz, ipso-C (PCy₃)), 36.7 (d, ³J_{PC} = 14 Hz, β-CH₂), 73.3 (s, α-CH₂), 113.7 (s, Cp), 125.6 (s, para-C), 127.6 (s, ortho-C), 129.7 (s, meta-C), 162.0 (s, ipso-C). ³¹P NMR (121 MHz, PhCl) δ 31.5 (s). ESI-MS (+ve detection) 707.3522 m/z [M]⁺, 353.2962 m/z [HO(C₄H₈)PCy₃]⁺.

Compound 8. Yield = 23 mg (65%). ¹H NMR (500 MHz, d₈-THF) δ 1.31 (9H, m, (CH₃)PEt₃), 1.70 (2H, m, β-CH₂ and γ-CH₂), 2.09 (6H, s, ortho-CH₃), 2.21 (3H, s, para-CH₃), 2.24 (2H, m, γ-CH₂), 2.27 (6H, m, (CH₂)PEt₃), 2.31 (2H, m, δ-CH₂), 4.10 (2H, t, ³J_{HH} = 6 Hz, α-CH₂), 6.23 (10H, s, Cp), 6.69 (2H, s, Ar-H). ¹³C NMR (125 MHz, d₈-THF) δ 5.62 (d, ²J_{PC} = 5 Hz, (CH₃)PEt₃), 12.1 (d, ¹J_{PC} = 49 Hz, (CH₂)PEt₃), 18.2 (s, ortho-CH₃), 18.9 (d, ¹J_{PC} = 45 Hz, δ-CH₂), 19.3 (d, ²J_{PC} = 5 Hz, γ-CH₂), 20.8 (s, para-CH₃), 36.2 (d, ³J_{PC} = 14 Hz, β-CH₂), 73.3 (s, α-CH₂), 113.7 (s, Cp), 125.6 (s, para-C), 127.6 (s, ortho-C), 129.7 (s, meta-C), 162.0 (s, ipso-C). ³¹P NMR (121 MHz, PhCl) δ 38.0 (s). ESI-MS (+ve detection) 545.2118 m/z [M]⁺, 191.1536 m/z [HO(C₄H₈)PEt₃]⁺.

Compound 9. Yield = 27 mg (68%). ¹H NMR (500 MHz, d₈-THF) δ 1.74 (2H, m, β-CH₂), 1.83 (2H, m, γ-CH₂), 2.01 (6H, s, ortho-CH₃), 2.16 (3H, s, para-CH₃), 3.40 (2H, m, δ-CH₂), 4.08 (2H, t, ³J_{HH} = 6 Hz, α-CH₂), 6.13 (10H, s, Cp), 6.67 (2H, s, Ar-H), 7.70–7.89 (15H, m, PPh₃). ¹³C NMR (125 MHz, d₈-THF): δ 17.8 (s, ortho-CH₃), 20.4 (d, ²J_{PC} = 5 Hz, γ-CH₂), 20.5 (s, para-CH₃), 22.6 (d, ¹J_{PC} = 51 Hz, δ-CH₂), 35.7 (d, ³J_{PC} = 16 Hz, β-CH₂), 72.7 (s, α-CH₂), 113.3 (s, Cp), 119.3 (d, ¹J_{PC} = 86 Hz, ipso-C (PPh₃)), 125.6 (s, para-C), 127.6 (s, ortho-C), 129.6 (s, meta-C), 131.2 (d, ³J_{PC} = 13 Hz, meta-C (PPh₃)), 134.3 (d, ²J_{PC} = 10 Hz, ortho-C (PPh₃)), 135.9 (d, ⁴J_{PC} = 3 Hz, para-C (PPh₃)), 161.6 (s, ipso-C). ³¹P NMR (121 MHz, PhCl) δ 23.4 (s). ESI-MS (+ve detection) 689.2124 m/z [M]⁺, 335.1563 m/z [HO(C₄H₈)PPh₃]⁺.

Synthesis of [Cp₂Zr(THF)OMes][B(C₆F₅)₄] (1-THF). In a glovebox, THF (0.25 mL) was added dropwise to a stirred chlorobenzene (1 mL) solution of 3 (40 mg, 0.4 mmol), resulting in a yellow solution. The product was isolated via precipitation into a large volume (25 mL) of rapidly stirred hexane. The resulting pale yellow powder was washed with pentane (3 × 5 mL) and dried in vacuo (37 mg, 86%). Crystals of 1-THF suitable for analysis by single crystal X-ray diffraction were obtained by layering a chlorobenzene solution with pentane (7 days).

¹H NMR (500 MHz, d₅-PhBr) δ 1.69 (4H, br s, THF (C₃,C₄)), 1.84 (6H, s, ortho-CH₃), 2.21 (3H, s, para-CH₃), 3.67 (4H, br s, THF (C₂, C₅)), 6.03 (10H, s, Cp), 6.76 (2H, s, Ar-H). ¹³C NMR (125 MHz, d₅-PhBr) δ 17.9 (s, ortho-CH₃), 20.7 (s, para-CH₃), 25.9 (br s, THF (C₃, C₄)), 77.8 (br s, THF (C₂, C₅)), 116.4 (s, Cp), 123.4 (s, ortho-C), 129.8 (s, meta-C), 160.9 (s, ipso-C). NB: All other peaks were obscured by the PhBr solvent.

Reactivity of [Cp*₂ZrOMes][B(C₆F₅)₄]/PR₃ (2a-e). In a glovebox, 2 (20 mg, 0.02 mmol) and an equimolar amount of the corresponding phosphine (a = PCy₃ (4.7 mg), b = PEt₃ (2.0 mg), c = PPh₃ (4.5 mg),

d = PMes₃ (6.6 mg), e = P(C₆F₅)₃ (9.0 mg)) were weighed out and dissolved in PhCl (0.7 mL) before transferring to an NMR tube fitted with a J. Young valve. The resulting solution was treated with five drops of THF and a slight lightening of the yellow color observed. The ³¹P NMR spectrum of the solution indicated full conversion to free phosphine in all cases caused by its displacement by the THF moiety. When the reaction was deemed complete by ³¹P NMR spectroscopy, the product was isolated by precipitation into rapidly stirred hexane, washed with pentane (3 × 5 mL), and dried in vacuo.

Compound 10. Yield = 13 mg, 51%. ¹H NMR (500 MHz, d₈-THF) δ 1.40–1.82 (30H, m, PCy₃), 1.91 (2H, m, β-CH₂), 2.31 (2H, m, δ-CH₂), 1.91 (30H, s, Cp*), 2.04 (3H, s, ortho-CH₃), 2.12 (3H, s, ortho-CH₃), 2.18 (3H, s, para-CH₃), 2.31 (2H, m, γ-CH₂), 4.27 (2H, m, α-CH₂), 6.55 (1H, s, Ar-H), 6.64 (1H, s, Ar-H). ¹³C NMR (125 MHz, *-Me), 16.3 (d, ¹J_{PC} = 43 Hz, δ-CH₂), 18.7 (s, d₈-THF), 111.8 (s, Cp para-CH₃), 19.9 (s, ortho-CH₃), 20.1 (d, ²J_{PC} = 5 Hz, γ-CH₂), 20.8 (s, ortho-CH₃), 26.4 (s, para-C(PCy₃)), 27.5 (d, ³J_{PC} = 13 Hz, meta-C(PCy₃)), 27.8 (d, ²J_{PC} = 4 Hz, ortho-C(PCy₃)), 30.8 (d, ¹J_{PC} = 43 Hz, ipso-C(PCy₃)), 38.2 (d, ³J_{PC} = 14 Hz, β-CH₂), 70.8 (s, α-CH₂), 121.3 (s, Cp*), 124.6 (s, para-C), 125.9 and 126.3 (s, ortho-C), 129.5 and 129.8 (s, meta-C), 158.0 (ipso-C). ³¹P NMR (121 MHz, PhCl) δ 33.9 (s). ESI-MS (+ve detection) 847.5089 m/z [M]⁺.

Compound 11. Yield = 18 mg, 78%. ¹H NMR (500 MHz, d₈-THF) δ 1.29 (9H, dt, ³J_{PH} = 18 Hz, ³J_{HH} = 7 Hz, CH₃(PEt₃)), 1.56 (2H, m, δ-CH₂), 1.89 (2H, m, β-CH₂), 1.91 (30H, s, Cp*), 2.04 (3H, s, ortho-CH₃), 2.12 (3H, s, ortho-CH₃), 2.18 (3H, s, para-CH₃), 2.24–2.32 (8H, m, γ-CH₂ and CH₂(PEt₃)), 4.27 (2H, m, α-CH₂), 6.55 (1H, s, Ar-H), 6.64 (1H, s, Ar-H). ¹³C NMR (125 MHz, d₈-THF) δ 5.62 (d, ²J_{PC} = 5 Hz, CH₃ (PEt₃)), 11.8 (s, Cp*-Me), 12.1 (d, ¹J_{PC} = 49 Hz, CH₂(PEt₃)), 18.4 (d, ¹J_{PC} = 47 Hz, δ-CH₂), 18.7 (d, ²J_{PC} = 4 Hz, γ-CH₂), 18.7 (s, para-CH₃), 19.9 (s, ortho-CH₃), 20.8 (s, ortho-CH₃), 37.6 (d, ³J_{PC} = 14 Hz, β-CH₂), 70.8 (s, α-CH₂), 121.3 (s, Cp*), 124.6 (s, para-C), 125.9 and 126.3 (s, ortho-C), 129.5 and 129.8 (s, meta-C), 158.0 (ipso-C). ³¹P NMR (121 MHz, PhCl) δ 36.8 (s). ESI-MS (+ve detection) 685.3691 m/z [M]⁺, 191.1540 [HO(C₄H₈)PEt₃]⁺.

Compound 12. Yield = 14 mg, 55%. ¹H NMR (500 MHz, d₅-PhBr). δ 1.78 (2H, m, δ-CH₂), 1.87 (30H, s, Cp*), 1.91 (2H, m, β-CH₂), 2.01 (3H, s, ortho-CH₃), 2.05 (3H, s, ortho-CH₃), 2.17 (3H, s, para-CH₃), 3.43 (2H, m, γ-CH₂), 4.21 (2H, m, α-CH₂), 6.53 (1H, s,

Ar-H), 6.63 (1H, s, Ar-H), 7.72–7.93 (15H, m, PPh₃). ¹³C NMR (125 MHz, d₅-PhBr) δ 11.7 (s, Cp*), 11.8 (d, ¹J_{PC} = 50 Hz, δ-CH₂), 18.7 (s, para-CH₃), 19.9 (s, ortho-CH₃), 20.8 (s, ortho-CH₃), 22.9 (d, ²J_{PC} = 4 Hz, γ-CH₂), 37.6 (d, ³J_{PC} = 15 Hz, β-CH₂), 70.7 (s, α-CH₂), 121.3 (s, Cp*), 128.7 and 129.5 (s, meta-C), 129.6 (d, ¹J_{PH} = 38 Hz, ipso-C (PPh₃)) 131.5 (d, ³J_{PC} = 11 Hz, meta-C (PPh₃)), 134.7 (d, ⁴J_{PC} = 4 Hz, para-C (PPh₃)), 157.9 (s, ipso-C). Ortho-C peak for the triphenylphosphine is obscured by the solvent. ³¹P NMR (121 MHz, PhCl) δ 22.2 (s). ESI-MS (+ve detection) 829.3684 m/z [M]⁺, 335.1563 m/z [HO(C₄H₈)PPh₃]⁺.

Synthesis of [Cp*₂Zr(THF)OMes]B(C₆F₅)₄ (2-THF). In a glovebox, THF (0.25 mL) was added dropwise to a stirred chlorobenzene (1 mL) solution of 2 (119 mg, 0.1 mmol), resulting in a yellow solution. The product was isolated via precipitation into a large volume (25 mL) of rapidly stirred hexane. The resulting pale yellow powder was washed with pentane (3 × 5 mL) and dried in vacuo (90 mg, 71%). Crystals of 2-THF suitable for analysis by single crystal X-ray diffraction were obtained by layering a chlorobenzene solution with pentane (7 days).

¹H NMR (500 MHz, d₅-PhBr) δ 1.59 (4H, s, THF (C3,C4)), 1.61 (30H, s, Cp*), 1.79 (3H, s, ortho-CH₃), 1.88 (3H, s, ortho-CH₃), 2.19 (3H, s, para-CH₃), 3.55 (4H, s, THF (C2, C5)), 6.03 (1H, s, Ar-H), 6.77 (1H, s, Ar-H). ¹³C NMR (125 MHz, d₅-PhBr) δ 10.2 (s, Cp*-Me), 17.0 (s, ortho-CH₃), 18.3 (s, ortho-CH₃), 20.1 (s, para-CH₃), 25.0 (s, THF (C3, C4)), 67.9 (s, THF (C2, C5)), 122.0 (s, Cp*), 129.4 (s, meta-C), 154.8 (s, ipso-C). NB: Remaining peaks in ¹³C NMR are obscured by the PhBr solvent.

4.8. Reaction of Pairs with Phenylacetylene (PhCCH). Reactivity of [Cp₂ZrOMes][B(C₆F₅)₄]/PR₃ (1a-e). In a glovebox, 1 (30 mg, 0.028 mmol) and an equimolar amount of the corresponding phosphine ((0.028 mmol, a = PCy₃ (8.1 mg), b = PEt₃ (3.4 mg), c = PPh₃ (7.6 mg), d = PMes₃ (11.3 mg), e = P(C₆F₅)₃ (15.4 mg)) were weighed out and dissolved in PhCl (0.7 mL) before transferring to an NMR tube fitted with a J. Young valve. Excess phenylacetylene (5 drops) was subsequently added, and in the case of 1a-d an instantaneous lightening of the yellow color was observed. The progress of the reactions was monitored by ³¹P NMR spectroscopy. Collected spectral data is detailed below:

1a. Reaction complete in <1 min. Mixture of products could not be sufficiently separated to allow further characterization. ³¹P NMR (121 MHz, PhCl) δ 33.2 (d, ¹J_{PH} = 430 Hz, H-PCy₃). ESI-MS (+ve detection) 281.2 m/z [HPCy₃]⁺.

1b. Reaction complete in 16 h. Mixture of products could not be sufficiently separated to allow further characterization. ³¹P NMR (121 MHz, PhCl) δ 25.5 (m, 1b-PhCCH), 30.3 (m, 1b-PhCCH). Proposed to be the two possible isomers of 1b-PhCCH. ESI-MS (+ve detection) 575.2 m/z [1b-PhCCH], 119.1 [HPEt₃]⁺.

1c. The reaction was seen to be complete after <1 min, and compound 13 was isolated in a glovebox by precipitation into rapidly stirred hexane (20 mL) and washed with pentane (3 × 5 mL) before drying in vacuo (27.3 mg, 69%). ¹H NMR (500 MHz, d₅-PhBr) δ 1.65 (6H, s, ortho-CH₃), 2.16 (3H, s, para-CH₃), 5.74 (10H, s, Cp), 6.66 (2H, s, Ar-H), 7.04 (2H, d, ³J_{HH} = 7 Hz, ortho-H (PhCCH)), 7.22 (2H, t, ³J_{HH} = 7 Hz, meta-H (PhCCH)), 7.32 (1H, t, ³J_{HH} = 7 Hz, para-H (PhCCH)), 7.25–7.42 (9H, m, meta/para-H (PPh₃)), 7.56

(3H, t, ³J_{HH} = 7 Hz, para-H (PPh₃)), 9.01 (1H, d, ³J_{PH} = 45 Hz, α-H). ¹³C NMR (125 MHz, d₅-PhBr) δ 21.4 (s, ortho-CH₃), 23.7 (s, para-CH₃), 115.2 (s, Cp), 122.6 (s, para-C), 126.6 (s, ortho-C), 132.5 (meta-C), 135.1 (s, ipso-C (PhCCH)), 137.1 (d, ³J_{PC} = 10 Hz, meta-C (PPh₃)), 137.9 (d, ⁴J_{PC} = 3 Hz, para-C (PPh₃)), 138.2 (d, ¹J_{PH} = 22 Hz, C-PPh₃), 163.2 (s, ipso-C), 212.6 (d, ³J_{PH} = 10 Hz, Zr-C(H)). ³¹P NMR (121 MHz, d₅-PhBr) δ 20.1 (s). NB: Remaining peaks in ¹³C NMR are obscured by the PhBr solvent. ESI-MS (+ve detection) 719.2015 m/z [M]⁺.

Reactivity of [Cp*₂ZrOMes][B(C₆F₅)₄]/PR₃ (2a-e). In a glovebox, 2 (20 mg, 0.017 mmol) and an equimolar amount of the corresponding phosphine (0.017 mmol, a = PCy₃ (4.7 mg), b = PEt₃ (2.0 mg), c = PPh₃ (4.5 mg), d = PMes₃ (6.6 mg), e = P(C₆F₅)₃ (9.0 mg)) were weighed out and dissolved in PhCl (0.7 mL) before transferring to an NMR tube fitted with a J. Young valve. Excess phenylacetylene (5 drops) was subsequently added, and in the case of

2a-d an instantaneous lightening of the yellow color was observed. The progress of the reactions was monitored by ³¹P NMR spectroscopy. Collected spectral data is detailed below:

2a. Reaction complete in <1 min. Mixture of products could not be sufficiently separated to allow further characterization. ³¹P NMR (121 MHz, PhCl) δ 20.1 (s, 2a-PhCCH, 38%), 33.2 (d, ¹J_{PH} = 450 Hz, HPCy₃, 62%). ESI-MS (+ve detection) 877.4 m/z [2a-PhCCH], 281.2 m/z [HPCy₃]⁺.

2b. Reaction complete in <1 min. Mixture of products could not be sufficiently separated to allow further characterization. ³¹P NMR (121 MHz, PhCl) δ 21.7 (d, ¹J_{PH} = 450 Hz, HPEt₃, 46%), 26.0 (s, 2b-PhCCH, 54%). ESI-MS (+ve detection) 715.4 m/z [2b-PhCCH], 119.1 [HPEt₃]⁺.

2c. The reaction was seen to be complete after <1 min, and compound 14 was isolated in a glovebox by precipitation into rapidly stirred hexane (20 mL) and washed with pentane (3 × 5 mL) before drying in vacuo (24.0 mg, 92%). Crystals of 14 suitable for analysis by single crystal X-ray diffraction were obtained by layering a PhCl solution of 14 with pentane (5 days). ¹H NMR (500 MHz, d₅-PhBr) δ 1.59 (30H, s, Cp*), 1.17 (3H, s, para-CH₃), 2.10 (3H, s, ortho-CH₃), 2.12 (3H, s, ortho-CH₃), 6.40 (2H, s, Ar-H), 7.50–7.76 (15H, m, PPh₃), 8.36 (1H, d, ³J_{PH} = 45 Hz, α-H). ¹³C NMR (125 MHz, d₅-PhBr) δ 15.4 (s, Cp*), 17.5 (s, para-CH₃), 22.9 and 23.6 (s, ortho-CH₃), 124.8 (Cp*), 128.1 (s, para-C), 131.7 (s, ortho-C), 132.5 (s, meta-C), 136.5 (d, ³J_{PH} = 14 Hz, meta-C (PPh₃)), 137.6 (d, ⁴J_{PH} = 4 Hz, para-C (PPh₃)), 158.9 (ipso-C), 233.1 (d, ³J_{PH} = 10 Hz, Zr-C(H)). ³¹P NMR (121 MHz, d₅-PhBr) δ 17.4 (d, ³J_{PH} = 48 Hz, 14). NB: Remaining peaks in ¹³C NMR are obscured by the PhBr solvent. ESI-MS (+ve detection) 859.3598 m/z [M]⁺.

2d. Reaction complete in <1 min. In situ analysis of the reaction mixture by ³¹P NMR spectroscopy showed clean conversion to deprotonation products; however, the zirconium acetylide complex could not be isolated cleanly. ³¹P NMR (121 MHz, PhCl) δ 28.7 (d, ¹J_{PH} = 476 Hz, [H-PMes₃]⁺, 100%).

2e. No reaction was evident by ³¹P NMR spectroscopy.

ASSOCIATED CONTENT

* Supporting Information

Additional experimental data: DOSY spectra, NMR spectra, and X-ray diffraction data (PDF)
Crystallographic data (CIF)

AUTHOR INFORMATION

Corresponding Author

*duncan.wass@bristol.ac.uk

Notes

The authors declare no competing financial interest.

ACKNOWLEDGMENTS

O.J.M. would like to acknowledge Dr. Paul Gates and the University of Bristol Mass Spectrometry Service for their assistance and Dr. Craig Butts for his input on the DOSY experiments.

REFERENCES

- (1) (a) Stephan, D. W.; Erker, G. *Angew. Chem., Int. Ed.* 2015, 54, 6400. (b) Stephan, D. W. *J. Am. Chem. Soc.* 2015, 137, 10018.
- (2) (a) Stephan, D. W. *Acc. Chem. Res.* 2015, 48, 306. (b) (a) Welch, G. C.; Juan, R. S.; Masuda, J. D.; Stephan, D. W. *Science* 2006, 314, 1124. (b) Wang, X.; Kehr, G.; Daniliuc, C. G.; Erker, G. *J. Am. Chem. Soc.* 2014, 136, 3293. (c) Sajid, M.; Kehr, G.; Wiegand, T.; Eckert, H.; Schwickert, C.; Poettgen, R.; Cardenas, A. J. P.; Warren, T. H.; Fröhlich, R.; Daniliuc, C. G.; Erker, G. *J. Am. Chem.*

- Soc. 2013, 135, 8882–8895. (d) Scott, D. J.; Fuchter, M. J.; Ashley, A. E. *Angew. Chem., Int. Ed.* 2014, 53, 10218.
- (3) (a) Mömning, C. M.; Otten, E.; Kehr, G.; Fröhlich, R.; Grimme, S.; Stephan, D. W.; Erker, G. *Angew. Chem., Int. Ed.* 2009, 48, 6643. (b) Peuser, I.; Neu, R. C.; Zhao, X. X.; Ulrich, M.; Schirmer, B.; Tannert, J. A.; Kehr, G.; Fröhlich, R.; Grimme, S.; Erker, G.; Stephan, D. W. *Chem. - Eur. J.* 2011, 17, 9640. (c) Harhausen, M.; Fröhlich, R.; Kehr, G.; Erker, G. *Organometallics* 2012, 31, 2801. (d) Bertini, F.; Lyaskovskyy, V.; Timmer, B.; de Kanter, F.; Lutz, M.; Ehlers, A.; Slootweg, J.; Lammertsma, K. *J. Am. Chem. Soc.* 2012, 134, 201.
- (4) (a) Rosorius, C.; Kehr, G.; Fröhlich, R.; Grimme, S.; Erker, G. *Organometallics* 2011, 30, 4211. (b) Liedtke, R.; Fröhlich, R.; Kehr, G.; Erker, G. *Organometallics* 2011, 30, 5222. (c) Rosorius, C.; Daniliuc, C. G.; Fröhlich, R.; Kehr, G.; Erker, G. *J. Organomet. Chem.* 2013, 744, 149.
- (5) (a) Birkmann, B.; Voss, T.; Geier, S. J.; Ullrich, M.; Kehr, G.; Erker, G.; Stephan, D. W. *Organometallics* 2010, 29, 5310. (b) Welch, G. W.; Masuda, J. D.; Stephan, D. W. *Inorg. Chem.* 2006, 45, 478.
- (6) (a) Welch, G. C.; Stephan, D. W. *J. Am. Chem. Soc.* 2007, 129, 1880. (b) Spies, P.; Erker, G.; Bergander, K.; Fröhlich, R.; Grimme, S.; Stephan, D. W. *Chem. Commun.* 2007, 5072. (c) Mömning, C. M.; Otten, E.; Kehr, G.; Fröhlich, R.; Grimme, S.; Stephan, D. W.; Erker, G. *Angew. Chem., Int. Ed.* 2009, 48, 6643.
- (7) (a) Menard, G.; Stephan, D. W. *J. Am. Chem. Soc.* 2010, 132, 1796. (b) Appelt, C.; Westenberg, H.; Bertini, F.; Ehlers, A. W.; Slootweg, J. C.; Lammertsma, K.; Uhl, W. *Angew. Chem., Int. Ed.* 2011, 50, 3925. (c) Roters, S.; Appelt, C.; Westenberg, H.; Hepp, A.; Slootweg, J.; Lammertsma, K.; Uhl, W. *Dalton Trans.* 2012, 41, 9033. (d) Boudreau, J.; Courtemanche, M. A.; Fontaine, F. G. *Chem. Commun.* 2011, 47, 11131.
- (8) (a) Schafer, A.; Reissmann, M.; Schafer, A.; Saak, W.; Haase, D.; Muller, T. *Angew. Chem., Int. Ed.* 2011, 50, 12636. (b) Reißmann, M.; Schafer, A.; Jung, S.; Muller, T. *Organometallics* 2013, 32, 6736. (c) Herrington, T. J.; Thom, A. J. W.; White, A. J. P.; Ashley, A. E. *Chem. Commun.* 2012, 41, 9019. (d) Herrington, T. J.; Ward, B.; Doyle, L. R.; McDermott, J.; White, A. J. P.; Hunt, P. A.; Ashley, A. E. *Chem. Commun.* 2014, 50, 12753. (e) Scott, D. J.; Fuchter, M. J.; Ashley, A. E. *Angew. Chem., Int. Ed.* 2014, 53, 10218. (f) Scott, D. J.; Simmons, T. R.; Lawrence, E. J.; Wildgoose, G. G.; Fuchter, M. J.; Ashley, A. E. *ACS Catal.* 2015, 5, 5540. (g) Erős, G.; Mehdi, H.; Papai, I.; Rokob, T. A.; Kiraly, P.; Tarkanyi, G.; Soos, T. *Angew. Chem., Int. Ed.* 2010, 49, 6559. (h) Gyömöre, A.; Bakos, M.; Földes, T.; Papai, I.; Domjan, A.; Soos, T. *ACS Catal.* 2015, 5, 5366.
- (9) Flynn, S. R.; Wass, D. F. *ACS Catal.* 2013, 3, 2574.
- (10) Dehydrocoupling of amine-boranes has been achieved stoichiometrically with main group systems, but never in a catalytic sense. (a) Miller, A. J. M.; Bercaw, J. E. *Chem. Commun.* 2010, 46, 1709. (b) Whittell, G. R.; Balmond, E. I.; Robertson, A. P. M.; Patra, S. K.; Haddow, M. F.; Manners, I. *Eur. J. Inorg. Chem.* 2010, 3967. A single example of catalytic dehydrogenation has been reported however requires melt conditions Appelt, C.; Slootweg, J. C.; Lammertsma, K.; Uhl, W. *Angew. Chem., Int. Ed.* 2013, 52, 4256. In contrast, catalytic dehydrogenation of amine-boranes is very well-established for transition metal systems: see Leitao, E. M.; Jurca, T.; Manners, I. *Nat. Chem.* 2013, 5, 817 and references therein.
- (11) (a) Chapman, A. M.; Haddow, M. F.; Wass, D. F. *J. Am. Chem. Soc.* 2011, 133, 8826. (b) Chapman, A. M.; Haddow, M. F.; Wass, D. F. *J. Am. Chem. Soc.* 2011, 133, 18463. (c) Chapman, A. M.; Wass, D. F. *Dalton Trans.* 2012, 41, 9067. (d) Chapman, A. M.; Haddow, M. F.; Wass, D. F. *Eur. J. Inorg. Chem.* 2012, 2012, 1546.
- (12) (a) Xu, X.; Fröhlich, R.; Daniliuc, C. G.; Kehr, G.; Erker, G. *Chem. Commun.* 2012, 48, 6109. (b) Xu, X.; Kehr, G.; Daniliuc, C. G.; Erker, G. *J. Am. Chem. Soc.* 2013, 135, 6465.
- (13) (a) Neu, R. C.; Otten, E.; Lough, A.; Stephan, D. W. *Chem. Sci.* 2011, 2, 170. (b) Xu, X.; Kehr, G.; Daniliuc, C. G.; Erker, G. *Organometallics* 2013, 32, 7306. (c) Frömel, S.; Kehr, G.; Fröhlich, R.; Daniliuc, C. G.; Erker, G. *Dalton Trans.* 2013, 42, 14531.
- (14) Nishihara, Y.; Aoyagi, K.; Hara, R.; Suzuki, N.; Takahashi, T. *Inorg. Chim. Acta* 1996, 252, 91.
- (15) Stapleton, R. A.; Galan, B. R.; Collins, S.; Simons, R. S.; Garrison, J. C.; Youngs, W. J. *J. Am. Chem. Soc.* 2003, 125, 9246.
- (16) Tolman, C. A. *Chem. Rev.* 1977, 77, 313.
- (17) Rocchigiani, L.; Ciancaleoni, G.; Zuccaccia, C.; Macchioni, A. *J. Am. Chem. Soc.* 2014, 136, 112.
- (18) For further details on the experimental conditions employed, see the [Supporting Information](#).
- (19) Attempts to isolate 1a-CO₂, 1b-CO₂, 2a-CO₂, and 2b-CO₂ in an argon atmosphere resulted in decomposition to form [HPR₃][B(C₆F₅)₄] and an as yet unidentified zirconium containing species.
- (20) (a) Borkowsky, S. L.; Jordan, R. F.; Hinch, G. D. *Organometallics* 1991, 10, 1268. (b) Breen, B.; Stephan, D. W. *Inorg. Chem.* 1992, 31, 4019.
- (21) Intermolecular FLPs containing a transition metal have also been reported where the transition metal is purely present as an auxiliary and not as the Lewis acid. See Boone, M. P.; Stephan, D. W. *Chem. - Eur. J.* 2014, 20, 3333.
- (22) (a) Vatamanu, M. *Organometallics* 2014, 33, 3683. (b) Couturier, S.; Gautheron, B. J. *J. Organomet. Chem.* 1978, 157, 61.
- (23) Pangborn, A. B.; Giardello, M. A.; Grubbs, R. H.; Rosen, R. K.; Timmers, F. J. *Organometallics* 1996, 15, 1518.
- (24) Nilsson, M. J. *Magn. Reson.* 2009, 200, 296–302.